HHS Public Access

Author manuscript

Lipids. Author manuscript; available in PMC 2022 December 23.

Published in final edited form as:

Lipids. 2009 July ; 44(7): 631–641. doi:10.1007/s11745-009-3310-x.

Effect of Bilayer Phospholipid Composition and Curvature on Ligand Transfer by the α-Tocopherol Transfer Protein

Wen Xiao Zhang,
Department of Chemistry, Centre for Biotechnology, Brock University, 500 Glenridge Ave, St. Catharines, ON L2S 3A1, Canada

Grant Frahm,
Department of Chemistry, Centre for Biotechnology, Brock University, 500 Glenridge Ave, St. Catharines, ON L2S 3A1, Canada

Samantha Morley,
Department of Nutrition, School of Medicine, Case Western, Reserve University, Cleveland, OH 44106-4954, USA

Danny Manor,
Department of Nutrition, School of Medicine, Case Western, Reserve University, Cleveland, OH 44106-4954, USA

Jeffrey Atkinson
Department of Chemistry, Centre for Biotechnology, Brock University, 500 Glenridge Ave, St. Catharines, ON L2S 3A1, Canada

Abstract

We report here our preliminary investigations on the mechanism of α-TTP-mediated ligand transfer as assessed using fluorescence resonance energy transfer (FRET) assays. These assays monitor the movement of the model α-tocopherol fluorescent derivative ((*R*)-2,5,7,8-tetramethyl-chroman-2-[9-(7-nitro-benzo[1,2,5]oxadiazol-4-yl amino)-nonyl]-chroman-6-ol; NBD-Toc) from protein to acceptor vesicles containing the fluorescence quencher TRITC-PE. We have found that α-TTP utilizes a collisional mechanism of ligand transfer requiring direct protein–membrane contact, that rates of ligand transfer are greater to more highly curved lipid vesicles, and that such rates are insensitive to the presence of anionic phospholipids in the acceptor membrane. These results point to hydrophobic features of α-TTP dominating the binding energy between protein and membrane.

Keywords

α-Tocopherol; α-Tocopherol transfer protein; Lipid transfer protein; Membrane curvature; Unilamellar vesicles; LUV; SUV; FRET

jatkin@brocku.ca .

Electronic supplementary material The online version of this article (doi:10.1007/s11745-009-3310-x) contains supplementary material, which is available to authorized users.

Introduction

The human α-tocopherol transfer protein (α-TTP) is a soluble 32 kDa-protein chiefly expressed in the liver that is understood to be responsible for the selective retention of α-tocopherol from dietary sources over other forms of vitamin E [1]. This role is exemplified by mutant forms of the protein that are known to cause neurological deficits in persons having "ataxia with vitamin E deficiency" (AVED) [2–6]. It is further underscored by mice in which the *ttpA* gene has been deleted, that exhibit very low levels of plasma and tissue α-tocopherol [7–10] and present AVED-like neuropathological symptoms [11]. Despite these demonstrations of α-TTP centrality to tocopherol bioavailability and distribution, little is known about the molecular mechanism of α-tocopherol transport in hepatocytes, nor the means by which a-TTP assists in the re-secretion of a-tocopherol into the plasma where it is carried to extrahepatic tissues by plasma lipoproteins. For instance, while it is well documented that the majority of plasma tocopherol is carried by LDL and HDL, treatment of cultured hepatocytes with brefeldin A, which inhibits lipoprotein construction and secretion outside the cell, did not inhibit tocopherol secretion [12]. Similarly, mice in which the expression of liver microsomal triglyceride transfer protein (MTTP) is disrupted and thus do not secrete VLDL remain tissue-sufficient in tocopherol [13].

Lipid transfer proteins enable cells to transport hydrophobic compounds (e.g., fatty acids, phospholipids, sterols, retinoids, and α-tocopherol) across aqueous media inside cells. The means by which this is accomplished has been most thoroughly described for the fatty acid binding proteins (FABPs) that, in all cases except for the liver FABP [14, 15], bind directly to membrane surfaces where they extract or deliver their preferred ligand(s). In order to accomplish this task, FABPs take advantage of electrostatic forces between a collection of basic residues on an α-helical portal region and negatively charged membrane phospholipids [16].

In previous work using cultured hepatocyte cells it was shown [17, 18] that expressed α-TTP co-locates with a fluorescent form of α-tocopherol ((*R*)-2,5,7,8-tetramethyl-chroman-2-[9-(7-nitro-benzo[1, 2, 5]oxadiazol-4-yl amino)-nonyl]-chroman-6-ol; NBD-Toc) [19] in the late endosomal compartment. The localization of α-TTP to endosomes raises the possibility that the protein may prefer to associate with membranes of specific phospholipid composition, or defined curvature. We report here our investigations on the mechanism of α-TTP-mediated ligand transfer assessed using fluorescence resonance energy transfer (FRET) assays that monitor the movement of NBD-Toc from protein to acceptor vesicles. We have found that α-TTP utilizes a collisional mechanism of ligand transfer requiring direct protein–membrane contact, that rates of ligand transfer are greater for more highly curved lipid vesicles, and that such rates are insensitive to the presence of anionic phospholipids in the acceptor membrane.

Materials and Methods

Materials

Glutathione agarose and DNase I were purchased from Invitrogen (Burlington, ON, Canada). N-(6-tetra-methylrhodaminethio-carbamoyl)-1,2-dihexadecanoyl-*sn*-glycero-3-

phosphoethanol-amine, triethylammonium salt (TRITC-DHPE) was from Molecular Probes (Invitrogen, Oregon, USA). Thrombin was obtained from GE Healthcare (Piscataway, NJ, USA). RNase A and Triton X-100 were from Sigma (St. Louis, MI, USA). Polycarbonate membranes for lipid extrusion were purchased from Avestin, Inc (Ottawa, ON, Canada). The following phospholipids were obtained from Avanti Polar Lipids (Alabaster, AL, USA): Liver bovine L-α-phosphatidylcholine (liver PC), soy L-a-phosphatidylcholine (soy PC), porcine brain L-α-phosphatidylserine (PS), bovine liver phosphatidylinositol (PI), 1,2-dioleoyl-*sn*-glycerol-3-phosphocholine (DOPC), oleoyl lysobisphosphatidic acid (LBPA), and 1,2-dioleoyl-*sn*-glycerol-3-phosphate (DOPA). NBD-Toc was previously synthesized in our lab [19]. All other reagents were from BioShop Canada Inc. (Burlington, ON, Canada).

Protein Expression and Purification

Human α-TTP flanked by NotI and SalI restriction sites was subcloned into pGEX-4T-3 vector. This construct was transformed into *E. coli* BL21 (DE3) for protein expression [20]. *E. coli* cultures were grown in baffled flasks at 37 °C until OD 600 nm was between 0.4 and 0.6. The bacterial culture was cooled to room temperature before being induced with 400 μM IPTG. To improve the production of soluble α-TTP, the culture was grown at room temperature for 18 h. The cells were harvested and stored at −80 °C until use.

After being frozen and thawed three times, the *E. coli* pellet was re-suspended in buffer A (150 mM Tris pH 8.0, 150 mM NaCl, 1 mM EDTA, 10% glycerol, 0.1 mM DTT and 0.1 mM PMSF). Lysozyme (4 mg/ml) was added to the cell suspension and followed by 30 min incubation on ice. Nucleic acids were digested with the addition of 10 mM $MgCl_2$, DNase I (1,000 units/ml lysate) and RNase (50 μg/ml), followed by an additional 30 min incubation on ice. The cells were then homogenized and centrifuged at 40,000*g* for 30 min at 4 °C. The supernatant was applied to a glutathione affinity column, and nonspecific binding proteins were removed by 15 column volumes wash each of buffer B (Buffer A plus 0.5% Triton X and 10 mM $MgCl_2$) and buffer C (50 mM Tris, pH 8, 150 mM NaCl, 10 mM $MgCl_2$ and 0.1 mM DTT), respectively. On-column thrombin cleavage of GST-TTP was completed after 2 h of incubation at RT with 50 units of thrombin in PBS per 1 ml of resin. The α-TTP was eluted in buffer C and a final concentration of 0.5 mM PMSF was added to prevent further thrombin-induced degradation. GST bound on the column was eluted with PBS containing 20 mM glutathione, and the column was regenerated with 3 M NaCl in PBS. Each purified sample was subjected to SDS-PAGE analysis. The Bradford assay was used to determine protein concentration. Purified protein was stored at 4 °C and used within a few days after the purification. In general, α-TTP ligand transfer activity remained intact within 5 days of purification.

Lipid Vesicle Preparation

Acceptor lipid vesicles for ligand transfer assays contained 97 mol% PC and 3 mol% quencher TRITC-PE, unless otherwise specified. For anionic lipid vesicles, 15 mol% of indicated anionic phospholipid was incorporated in vesicle preparations. Chloroform was evaporated from lipid mixtures under a stream of N_2 and residual solvent removed by continued evaporation under 0.5 mmHg. Lipid mixtures were rehydrated in SET buffer (250 mM Sucrose, 100 mM KCl, 50 mM Tris, 1 mM EDTA, pH 7.4). The lipid suspensions

were vortexed and incubated for 30 min at room temperature before liposome preparation. Large unilamellar vesicles (LUV) were prepared with a Liposofast mini-extruder (Avestin, Inc.). Briefly, lipid suspensions were extruded through a polycarbonate membrane (100-nm membrane for standard LUV preparation) for 15 passages to produce uniform size LUV. Small unilamellar vesicles (SUV) were prepared, following the procedure described by Schroeder and Thompson [21] with minor modifications. Briefly, lipid suspensions were sonicated using a titanium microprobe and a W-375 cell disruptor (Heat Systems-Ultrasonic, Inc.). Lipid samples were sonicated on ice for 45 min with output setting level of 2.5 and 35% duty cycle. The resulting liposomes were centrifuged at 110,000*g* for 2 h at 4 °C to remove large vesicles and titanium particles. To compare the difference between probe and bath sonicated SUV, SUV were also prepared by sonication for 45 min with a Branson bath sonicator Model 2510 (Branson, USA). SUV produced from both methods appeared to behave similarly toward α-TTP mediated tocopherol transfer. Ideally, a phosphorous assay should be performed to determine the phospholipid concentration after each vesicle preparation. However, due to the presence of a high sucrose content in the SET buffer, lipid samples turned black during acidic digestion at 190 °C, and thus such assays could not be used regularly to assess phospholipid concentration. To confirm that there is no loss of phospholipids due to extrusion and sonication procedures, the phosphorous assay was performed initially with SET buffer without sucrose, and the result suggested that the lipid concentration remains the same before and after the preparation. For the experiments that compared the vesicles of different size, the same rehydrated lipid mixture (multilamellar vesicles) was used to generate SUVs or LUVs of the same stock concentration. An estimation of vesicle concentration can be determined based on the emission spectrum of quencher TRITC-PE at approximately 575 nm. Lipid samples were prepared freshly for each experiment.

We measured the size of all lipid vesicles using a single angle (90°) quasi-elastic light scattering (QELS) instrument (Bookhaven Instruments Corporation) with a Melles Griot HeNe Laser (35 mW, 632.8 nm) and BI-APD 8590 digital auto-correlator. A cumulative statistical method was used to calculate particle size distributions. We found that all vesicles have nominal diameters larger than expected from the pore size of the filters when the extrusion method is used. We also note that the sucrose-containing buffer elicited a significant background signal that led to an overestimation of the size of small vesicles. Increased vesicle size has been seen previously with vesicles made in sucrose-containing buffers [22]. In general, the size variation is larger than expected for smaller vesicles than for bigger ones.

The average diameters of vesicles (nm) and their polydispersity index (in parentheses) were, by probe sonication; 106 nm (0.283), bath sonication; 134 nm (0.262); and by extrusion through polycarbonate filters of nominal pore size 30 nm (91 nm, 0.122), 50 nm (107 nm, 0.119), 100 nm (158 nm, 0.116), and 200 nm (219, 0.103). When vesicles of expected size 100 nm were prepared in Tris buffer rather than SET, the average size was 114 nm (0.085) emphasizing the overestimation of vesicle size that occurs in SET buffer.

We also separately determined the size of the smallest vesicles we prepared by sonication and extrusion on a DyanProTM NanoStar (Wyatt Technology). In this case probe sonication

gave vesicles of an average size of 67 nm (polydispersity 0.326) and extruded vesicles using 30 nm filters, 55 nm (0.034).

Partition Coefficient of NBD-Toc Between α-TTP and PC Lipid Vesicles

Kinetic analyses of FRET-based ligand transfer assays are only useful if the transfer is essentially unidirectional. In this work we have monitored the decrease in fluorescence intensity as NBD-Toc bound to α-TTP (where the signal is high) is transferred to PC vesicles containing the quencher TRITC-PE (where the signal is low). In order to be assured of unidirectional transfer, the partition coefficient (K_p) of NBD-Toc between α-TTP and vesicles must be known. Once K_p is known, appropriate concentrations of donor protein-ligand complex and acceptor vesicles can be chosen. The K_p of NBD-Toc was measured following literature procedures for fluorescent fatty acid transfer from albumins and FABPs to lipid vesicles [15, 23]. Briefly, several solutions were prepared containing a 9:1 ratio of α-TTP:NBD-Toc (final protein and ligand concentrations were 1 lM αTTP:0.1 μM NBD-Toc in SET, pH 7.4) that assured the absence of appreciable amounts of free NBD-Toc. (The K_d of NBD-Toc for α-TTP was determined to be between 8.5 [24] and 56 nM [19] depending on the assay conditions and whether the α-TTP used was a GST or Histagged fusion. Natural α-tocopherol has a K_d of 25 nM using a tritiated-tocopherol binding assay [25]). These high affinities of the protein for the ligand suggest that the α-TTP concentrations for both kinetic and partitioning experiments are sufficient to bind all available NBD-Toc. The samples were incubated for 15 min with gentle rotation. To each of these solutions were added amounts of LUVs or SUVs containing TRITC-PE (measured as μM total phospholipid) so that the final lipid concentration ranged from 50 to 400 μM. The resulting mixture was incubated for 15 min to allow NBD-Toc to equilibrate between α-TTP and acceptor SUVs or LUVs, the fluorescence spectrum of NBD-Toc from 475 to 600 nm was recorded, and the changes in the fluorescence at 520 nm were applied to the following equation [23, 26] to calculate partition coefficients:

$$1/\Delta F = 1/K_p(1/\Delta F_{max})(mol\alpha - \text{TTP/mol PC}) + 1/\Delta F_{max} \quad (1)$$

where ΔF is the difference between the initial fluorescence of NBD-Toc bound to α-TTP and the fluorescence at a given protein/PC ratio, and ΔF_{max} is the maximum fluorescence change [15]. A plot of $1/\Delta F$ versus $(1/\Delta F_{max})$ (mol α-TTP/mol PC) gave a straight line whose slope was equal to $1/K_p$.

Transfer of NBD-Toc to Lipid Vesicles Investigated by FRET

The rate of NBD-Toc transfer from α-TTP to lipid vesicles was investigated utilizing a FRET assay. Experiments were performed using a Photon Technologies, Inc. QuantaMaster-QM-2001–4 fluorometer (Photon Technologies International, Inc.) equipped with SPF-17 stopped-flow device which were used to determine the kinetics of NBD-Toc transfer to quencher TRITC-PE containing acceptor vesicles. The emission spectrum of NBD-Toc overlaps with the excitation spectrum of TRITC-PE, thus, upon mixing of donor (a-TTP bound NBD-Toc) and acceptor (TRITC-PE containing vesicles), the fluorescence intensity decreases with time. The excitation and emission wavelengths used were 466 and 526

nm, respectively. Standard transfer experiments were performed by incubating 0.45 μM NBD-Toc with 4 μM α-TTP for 15 min prior to mixing with 200 μM acceptor vesicles using the SPF-17 stopped-flow device. The final concentrations after mixing were 0.225 μM NBD-Toc, 2 μM α-TTP and 100 μM vesicles. The ratio of α-TTP to NBD-Toc was kept at 9:1 to ensure that there was no free ligand and that the fluorescence signal was solely attributed to protein-bound NBD-Toc. A 50-fold excess of acceptor vesicle was used based on the partition coefficient of NBD-Toc between α-TTP and vesicles. All experiments were performed at 20 °C. The fluorescence quench was monitored over time and normalized to the starting fluorescent intensity of NBD-Toc bound to α-TTP as 100%. To study the intervesicular transfer of NBD-Toc, 1 mol% of NBD-Toc was incorporated into PC SUV or LUV, and the transfer of NBD-Toc from these vesicles to PC LUV or SUV were monitored. In our assay condition, after subtraction of the signal due to slight ligand photobleaching, the rate of NBD-Toc transfer was best fitted with a single exponential decay Eq. 2 provided by Prism software (version 5, GraphPad Software, Inc., El Camino Real, San Diego, CA, USA).

$$y = (y_0 - y_{\text{inf}}) * \exp(-k * x) + y_{\text{inf}} \quad (2)$$

where y_0 is the initial fluorescence when NBD-Toc bound to α-TTP, k is the rate constant, x is the half time, and y_{inf} is the remaining fluorescence signal after NBD-Toc has been transferred to the acceptor vesicle, which in our case is approximately 55% of the original fluorescence signal.

Results

A representative determination of the partition coefficient of NBD-Toc between α-TTP and vesicles of different size is shown in Fig. 1. The slopes of the lines for both LUVs and SUVs over this lipid concentration range are very similar and shallow. The average values of the determined partition coefficient, K_p, of NBD-Toc between α-TTP and bovine liver phosphatidylcholine unilamellar vesicles were determined to be 0.064 ± 0.026 (n = 4) for LUVs and 0.098 ± 0.035 (n = 3) for SUVs. These values are not significantly different from each other. As the units of K_p are (mol lipid-bound NBD-Toc/mol phospholipid)/(mol protein-bound NBD-Toc/mol protein) the magnitude of K_p shows that NBD-Toc binds to α-TTP with ~10–15 times greater affinity than to lipid. Thus, for our transfer assay conditions to reflect unidirectional movement from protein to vesicle, an excess of phospholipids must be provided. Our assays use a 50-fold molar excess of phospholipids over α-TTP and represent a convenient concentration that assures unidirectional transfer, is not wasteful of phospholipids, and maintains the rate of transfer within the kinetic window of our stopped-flow device (mixing dead time ~20 ms). At equilibrium, the assays show a ~50% loss of the original fluorescence from protein-bound NBD-Toc.

However, it was observed that spontaneous intervesicular ligand transfer in the absence of α-TTP occurred at a higher rate for donor SUVs than donor LUVs (Fig. 2). Note that the fastest observed rate was for movement of NBD-Toc from donor SUV to acceptor SUV; when the donor vesicles were LUVs the rates were lowered by about 50%. This may represent a combination of the enhanced water-solubility of NBD-Toc (calculated log P = 7.34) compared to natural α-tocopherol (log P = 9.60), and the ease of ligand

movement from the differing lipid packing of SUVs and LUVs. Our previous work with NBD-tocopherol in hepatocytes [17, 18] showed that this ligand partitions to membranes and that residence time in mainly endosomal membranes is dependent on the inducible expression of TTP that clears the fluorescence signal from the cell. This behavior completely mimics similar secretion assays done using ^{14}C-α-tocopherol. Furthermore, we recently reported on the effect of tocols on aspects of membrane curvature using differential scanning calorimetry (DSC) [27]. All of the tocopherols and tocotrienols lowered both the gel to liquid crystalline transition temperature (T_M) and the liquid crystalline to inverted hexagonal transition (T_H) of dielaidoyl phosphatidylethanolamine. We have repeated such measurements with NBD-α-tocopherol and found them to be more similar to natural α-tocopherol than any other tocol. In the above-cited work, the numbers for α-tocopherol were: ΔT_M (°C/mol fraction) = −41 ± 4 and ΔT_H (°C/mol fraction) = −300 ± 35. The values for NBD-α-tocopherol were ΔT_M = −33 ± 4 and ΔT_H = −262 ± 17, suggesting that NBD-tocopherol has the same effect on the physical attributes of a membrane as does α-tocopherol.

To test whether α-TTP uses a collisional mechanism of transfer where membrane binding is required [16], the concentration of acceptor phospholipids was increased while keeping the protein:ligand concentration constant. If protein–membrane collision is required then the rate of transfer should increase with increasing concentration of phospholipid. As shown in Fig. 3, the rate of transfer of NBD-Toc from α-TTP is quite insensitive to LUV concentration. However, the rates did increase about 50% (0.011 ± 0.0017–0.017 ± 0.005 s^{-1}) when the LUV concentration was increased from 50 to 750 μM. When SUVs were the ligand acceptor the enhancement of transfer was much more dramatic as the lipid amount was raised, increasing ~4.5-fold from 25 to 625 μM phospholipids. Indeed, we have noted a 4-nm red-shift of the intrinsic tryptophan fluorescence of α-TTP when bound to PC SUVs [28] suggesting that α-TTP binding to these vesicles is accompanied by a significant environmental change around tryptophan residues.

Supporting evidence for a collisional versus diffusional mechanism can be obtained if the rate of transfer is not affected by an increase in ionic strength of the medium. High ionic strength slows the rate of transfer if the ligand must first leave the protein and diffuse to a nearby membrane. Hydrophobic compounds such as α-tocopherol and NBD-Toc, which already have very low aqueous solubility, would be even less likely to exist free in buffer due to the increased solvent polarity of the high salt buffer. This has been demonstrated for the liver FABP [15]. Figure 4 shows that there is no transfer rate reduction for movement of NBD-Toc from α-TTP to SUVs (100% PC or 15 mol% PS in PC) up to 1.0 M salt.

We hypothesized that α-TTP would show enhanced rates of ligand transfer to membranes that contained anionic lipids, since this has been noted for other lipid transfer proteins such as the FABPs [26, 29–32], and cellular retinol binding protein I [33]. However, when SUVs were prepared containing 15% of anionic phospholipids such as bovine liver PI, DOPS, LBPA, or DOPA, rates of NBD-Toc transfer by α-TTP showed only minor rate variations (Fig. 5). An increase in the concentration of PS from 15 to 25% did not significantly increase the observed rate. Transfer rates from TTP to LUV were 4–10 times slower than for SUVs (data not shown). Inclusion of 15% cholesterol in bovine liver PC vesicles (both

SUV and LUV) had no effect on the rate of transfer when compared to vesicles without cholesterol. The greater rate of transfer to SUV over LUV was, however, maintained (data not shown).

To explore further the effect of membrane surface curvature, vesicles of differing size were prepared by liposome extrusion through specific pore size filters and by sonication. The rates of NBD-Toc transfer to PC vesicles of 50-, 100-, or 200-nm diameters were similar (k = ~0.017 ± 0.0009 s^{-1}, Fig. 6). Sonicated vesicles, using either an immersion probe or bath sonicator, are generally accepted to yield SUVs of about ~25 nm in diameter [34, 35] and consistently showed 5–7 fold faster rates of ligand transfer than larger vesicles. For the probe-sonicated vesicles the rate was 0.114 ± 0.023 s^{-1} and for bath sonicated was 0.098 ± 0.005 s^{-1}.

To assess the influence of lipid packing on the transfer process, the rate of NBD-Toc transfer to acceptor phospholipid vesicles of differing degrees of unsaturation is shown in Fig. 7. Three different sources of phosphatidylcholine were tested: soy PC (that has a saturated to unsaturated lipid ratio (S/U) of 0.30 and is composed predominantly 18:2 acyl chains; synthetic dioleoylphosphatidylcholine (DOPC); and bovine liver PC (which has a S/U ratio of 0.91). (Product data from Avanti Polar Lipids, Alabaster, AL). The rates of α-TTP mediated ligand transfer were faster to SUV than LUV acceptors, and soy PC lipids that contain a larger fraction of unsaturated acyl chains supported a transfer rate twice as fast as either DOPC or bovine liver PC.

Discussion

The α-tocopherol transfer protein is one important mechanism for the selective retention of α-tocopherol over other forms of vitamin E found in the diet. The selectivity of α-tocopherol binding to a-TTP [25, 36], coupled with enhanced oxidative metabolism of non-α-tocols [37, 38], explains how plasma levels of α-tocopherol exceed those of γ-tocopherol for North Americans despite the dietary surplus of γ-tocopherol [39]. Once bound to α-TTP, α-tocopherol is secreted from hepatocytes by an as yet unknown mechanism, and carried in plasma by lipoproteins [1, 40, 41].

α-TTP is a soluble protein that is assumed to bind peripherally to membranes given its localization to late endosomes [18] and it ability to bind phospholipid vesicles in vitro [28]. The membrane-binding characteristics of peripheral membrane proteins are known to combine both electrostatic interactions and hydrophobic forces [42]. Proteins that depend chiefly on the presence of anionic phospholipids such as PS for favorable membrane binding include lipopolysaccharide binding protein (LBP) [43, 44], and bactericidal/permeability-increasing protein (BPI) [45, 46]. BPI (a family member along with PLTP and LBP) has a group of basic residues on its amino terminus that are responsible for recognition of acidic sites on bacterial endotoxin. The fatty acid binding proteins (FABPs) also have a cluster of basic residues on the loop capping the binding cavity that are key to their recognition of anionic membranes [16, 26, 29]. Figure 5 shows that when anionic lipids were incorporated at 15 mol% (and 25% PS) there was no effect on the rate of ligand transfer to SUV or LUVs. It remains possible that more significant differences might be apparent at much

higher anionic lipid concentration, but we chose to use 15 mol% of these lipids since PI, PA, and LBPA rarely if ever occur in concentrations higher than this.

Other proteins have been shown to rely more on hydrophobic surface penetration into the lipid bilayer. The human phospholipid transfer protein (PLTP) uses a hydrophobic patch in the N-terminal tip of the protein for membrane binding. Mutations of these residues showed reduced binding [47]. Other contributions of hydrophobic residues for membrane binding have been noted for bee venom secreted PLA_2 [48] and human group × secreted PLA_2 [49, 50].

A protein that uses predominantly hydrophobic interactions for membrane binding would presumably have difficulty arriving at any specific cellular bilayer membrane since all bilayers contain a hydrophobic core. Many proteins are directed to membranes that contain specific lipids such as the phosphatidylinositol phosphates (PIPs) through protein motifs such as the FYVE and PX domains that specifically recognize these anionic lipids [51–54]. Indeed, it has been recently noted that α-TTP may also have some specificity for membranes containing PIPs even though α-TTP does not contain a FYVE or PX domain [55].

Bilayer curvature is also a variable in membrane recognition and binding by proteins. Biological membranes are in constant flux, undergoing fusion, exo- and endocytosis processes, all of which generate areas of high curvature and/or curvature stress [56–58]. The size of the organelle thus does not necessarily reflect local membrane curvature or curvature stress since such forces can occur in local portions of larger membranes [59].

α-TTP is known to localize to late endosomes [17, 60], structures that have complex membrane dynamics and topology [61–63]. Late endosomes occur in dense tubular, multi-lamellar, and multi-vesicular subclasses [64] and are reported to be 200–750 nm in diameter [64–66]. The endosome-specific phospholipid LBPA (lysobisphosphatidic acid, also known as bis(monoacylglycero)phosphate, BMP) [67, 68] appears key to multivesicular body (MVB) structure and function. The interior vesicles of the MVB (called “exosomes” as they are destined for exocytosis) are “pinched” from the MVB limiting membrane at sites rich in LBPA and lysolipids that, at low pH, stabilize this highly curved membrane substructure [69]. The exosomes, however, are not enriched in LBPA [70]. α-TTP has been shown to co-localize with LBPA in rat McARH7777 cells transfected with α-TTP [71]. Our results suggest that this is not due to a specific attraction of α-TTP for LBPA, but rather the effect of LBPA on the properties of the endosomal membrane and the pH-dependent formation of the highly curved MVB [72–74]. The failure of LBPA to enhance α-TTP transfer of NBD-Toc in our assays may be due to lack of an internal acidic pH as in MVBs or, more likely, that SUVs—whether they contain LBPA or not—already have sufficient membrane curvature to enhance in vitro α-TTP binding and thus ligand transfer. Therefore, the co-localization of α-TTP with LBPA [71] may be a secondary effect (high curvature) rather than due to a direct interaction of α-TTP with LBPA. Contrarily, the Niemann-Pick-type C2 protein that also occurs in endosomes has recently been shown to exhibit enhanced cholesterol transfer in the presence of SUVs containing 25% anionic lipids such as PI and PS, but is most pronounced in the presence of LBPA [75].

The sensitivity of membrane binding proteins to bilayer curvature is common. For example, an increased rate of ligand transfer from protein to SUVs over LUVs has been observed previously for FABPs [30, 76, 77]. The binding of sterol carrier protein 2 [78], and the glycolipid transfer protein (GLTP) [79] have also been shown to favor more highly curved membranes. The lipid-packing sensor of Arf GTPase activating protein 1 (arfGAP1) known as ALPS2, also preferentially binds to the more highly curved surface of SUVs [80, 81].

Wootan and Storch [82] observed faster rates of fluorescent fatty acid transfer from adipocyte and heart fatty acid bind protein (A- and H-FABP) to SUVs. They noted that this may be due to the greater number of SUVs versus LUVs prepared from an equal amount of lipid, and suggested that this could be the prime reason for the approximately ten-fold greater rate for transfer to SUVs than LUVs. We observed approximately the same increased rate of transfer to extruded 30 nm vesicles (~5-fold) and sonicated vesicles (~11-fold) as did Wootan and Storch. These authors also noted, however, that tighter packing of the phospholipid acyl chains in LUV due to their more flat lamellar structure may also have decreased rates of ligand transfer to LUVs. Our preparation of vesicles of different size used equal molar amounts of phospholipids. If we assume that vesicles are of uniform size and unilamellar, that the membrane thickness is ~5 nm, and that the area per phospholipid (here assumed to be DOPC) is 67.4 nm^2 [83], then the total available surface area for protein lipid interaction can be calculated (See Supplementary Material). The area available on the outer leaflet of vesicles increases by only 1.5 times when vesicle size is reduced from 200 to 20 nm when an equal amount of phospholipid is used for all samples. If the rate of ligand transfer was determined solely by the available surface area, we should have seen no more than an ~1.5 fold increase in transfer rate as vesicle size was varied from the larger 200 nm LUVs to smaller SUVs. However, we repeatedly saw transfer rate increases of ~11-fold on moving from extruded LUVs, to SUVs prepared by either extrusion or sonication, substantiating that TTP prefers to bind to SUV membranes of higher curvature.

It is worth noting that the spontaneous rates of NBD-tocopherol transfer between vesicles shown in Fig. 2 clearly shows that LUVs are both poorer donors and acceptors of NBD-tocopherol. Coupling this with our previous observation that TTP binds much better to SUVs than LUVs [28], suggests that in fact, the transfer of NBD-tocopherol to SUVs is faster due to the ease of both protein and ligand insertion into the membrane.

The collisional insertion of a ligand into a membrane by a protein can, in theory, be broken into two discrete steps: (1) binding of the protein-ligand complex to the acceptor membrane, and (2) insertion of the ligand into the bulk of the membrane. Our results do not rule out the possibility that ligand insertion occurs at different rates when the membrane structure is perturbed. However, the spontaneous rate of ligand movement from LUV donors to SUV or LUV acceptors suggests that NBD-Toc (as a model of α-tocopherol) inserts equally well into both membrane types. The presence of anionic lipids could enhance protein binding through electrostatic interactions between the protein and the phospholipid head group, or it might make ligand insertion easier if the anionic phospholipids have changed the packing density of the membrane. The present work cannot rule out packing density changes in the acceptor membrane, but the fact that each anionic phospholipid supported near equal

transfer rates whether they are present in SUVs or LUVs suggests that packing is not an important variable in rates of NBD-Toc transfer by α-TTP.

The only phospholipid composition that changed the rate of NBD-Toc transfer to vesicles by α-TTP were soy PC lipids. The higher degree of unsaturation in these plant lipid samples may provide a more receptive membrane environment for tocopherol as it is well-known that tocols prefer to partition into those phospholipid phases that are rich in polyunsaturated lipids [27].

In this report we have used only the wild type α-TTP to explore the variables that affect the rates of ligand movement from protein to membrane. The lack of effect of anionic phospholipids suggests that membrane recognition may rely more on hydrophobic forces, something that has been well interpreted by several comprehensive surveys [84–88]. We have now begun studies with mutant forms of α-TTP that perturb the putative hydrophobic face of the protein that is offered to membranes. We will soon report their ability to bind membranes and effect ligand transfer.

The α-TTP is selective for more highly curved membranes as observed by its fast transfer of NBD-Toc to small unilamellar vesicles of ~25 nm diameter versus vesicles of diameter larger than ~50 nm, but does not show any preference for anionic lipids when binding membranes. This preference for highly curved membranes may be linked to the localization of α-TTP to the late endosomes whose membranes are quite dynamic, and form small internal vesicles with the aid of the endosome-specific phospholipid LBPA. The degree of phospholipid unsaturation may also be a controlling feature for delivery of tocopherol to membranes since the plant-derived soy PC supported faster ligand transfer than did pure DOPC or bovine liver PC, both of which have a lower unsaturation content.

Supplementary Material

Refer to Web version on PubMed Central for supplementary material.

Acknowledgment

We thank Richard and Raquel Epand (Bio-chemistry, McMaster University) for the DSC measurements with NBD-α-tocopherol; Doug Keller and Yuguo Cui (Chemical Engineering, McMaster University) and Sigrid Kuebler (Wyatt Technology Corporation) for measurement of vesicle sizes. This work was supported by a grant from the Natural Sciences and Engineering Research Council of Canada to J.A. and, in part, by award DK067494 to D.M.

Abbreviations

AVED	Ataxia with vitamin E deficiency
DOPA	Dioleoylphosphatidic acid
DOPC	Dioleoylphosphatidylcholine
EDTA	Ethylenediaminetetraacetic acid
FABP	Fatty acid binding protein

FRET	Fluorescence resonance energy transfer
HDL	High density lipoprotein
LBPA	Lysobisphosphatidic acid
LDL	Low density lipoprotein
LUV	Large unilamellar vesicle
MVB	Multivesicular body
NBD-Toc	(*R*)-2,5,7,8-tetramethyl-chroman-2-[9-(7-nitro-benzo[1,2,5]oxadiazol-4-yl amino)-nonyl]-chroman-6-ol
PC	Phosphatidylcholine
PE	Phosphatidylethanolamine
PI	Phosphatidylinositol
PIPs	Phosphoinositide phosphates
PMSF	Phenylmethanesulfonyl fluoride
PS	Phosphatidylserine
POPC	1-Palmitoyl-2-oleoyl phosphatidylcholine
PUFA	Polyunsaturated fatty acid
SUV	Small unilamellar vesicle
TRITC-PE	*N*-(6-tetramethylrhodaminethio-carbamoyl)-1,2-dihexadecanoyl-*sn*-glycero-3-phosphoethanol-amine, triethylammonium salt
VLDL	Very low density lipoprotein

References

1. Manor D, Morley S (2007) The alpha-tocopherol transfer protein.Vitam Horm 76:45–65 [PubMed: 17628171]
2. Federico A (2004) Ataxia with isolated vitamin E deficiency: atreatable neurologic disorder resembling Friedreich's ataxia. Neurol Sci 25:119–121 [PubMed: 15300458]
3. Hoshino M, Masuda N, Ito Y, Murata M, Goto J, Sakurai M, Kanazawa I (1999) Ataxia with isolated vitamin E deficiency: a Japanese family carrying a novel mutation in the alpha-tocopherol transfer protein gene. Ann Neurol 45:809–812 [PubMed: 10360777]
4. Cavalier L, Ouahchi K, Kayden HJ, Di Donato S, Reutenauer L, Mandel JL, Koenig M (1998) Ataxia with isolated vitamin E deficiency: heterogeneity of mutations and phenotypic variability in a large number of families. Am J Hum Genet 62:301–310 [PubMed: 9463307]
5. Ouahchi K, Arita M, Kayden H, Hentati F, Ben Hamida M, Sokol R, Arai H, Inoue K, Mandel J, Koenig M (1995) Ataxia with isolated vitamin E deficiency is caused by mutations in the alpha-tocopherol transfer protein. Nat Genet 9:141–145 [PubMed: 7719340]

6. Hentati A, Deng H, Hung W, Nayer M, Ahmed M, He X, Tim R, Stumpf D, Siddique T (1996) Human alpha-tocopherol transfer protein: gene structure and mutations in familial vitamin E deficiency. Ann Neurol 39:295–300 [PubMed: 8602747]
7. Nishida Y, Yokota T, Takahashi T, Uchihara T, Jishage KI, Mizusawa H (2006) Deletion of vitamin E enhances phenotype of Alzheimer disease model mouse. Biochem Biophys Res Commun 350:530–536 [PubMed: 17026966]
8. Leonard SW, Terasawa Y, Farese RV, Traber MG (2002) Incorporation of deuterated RRR- or all-rac-alpha-tocopherol in plasma and tissues of alpha-tocopherol transfer protein-null mice. Am J Clin Nutr 75:555–560 [PubMed: 11864863]
9. Jishage K, Arita M, Igarashi K, Iwata T, Watanabe M, Ogawa M, Ueda O, Kamada N, Inoue K, Arai H, Suzuki H (2001) alpha-tocopherol transfer protein is important for the normal development of placental labyrinthine trophoblasts in mice. J Biol Chem 276:1669–1672 [PubMed: 11076932]
10. Terasawa Y, Ladha Z, Leonard SW, Morrow JD, Newland D, Sanan D, Packer L, Traber MG, Farese RV (2000) Increased atherosclerosis in hyperlipidemic mice deficient in alpha-tocopherol transfer protein and vitamin E. Proc Natl Acad Sci USA 97:13830–13834 [PubMed: 11095717]
11. Yokota T, Igarashi K, Uchihara T, Jishage K, Tomita H, Inaba A, Li Y, Arita M, Suzuki H, Mizusawa H, Arai H (2001) Delayed-onset ataxia in mice lacking alpha-tocopherol transfer protein: Model for neuronal degeneration caused by chronic oxidative stress. Proc Natl Acad Sci USA 98:15185–15190 [PubMed: 11752462]
12. Arita M, Nomura K, Arai H, Inoue K (1997) a-Tocopherol transfer protein stimulates the secretion of a-tocopherol from a cultured liver cell line through a brefeldin A-insensitive pathway. Proc Natl Acad Sci USA 94:12437–12441 [PubMed: 9356467]
13. Minehira-Castelli K, Leonard SW, Walker QM, Traber MG, Young SG (2006) Absence of VLDL secretion does not affect alpha-tocopherol content in peripheral tissues. J Lipid Res 47:1733–1738 [PubMed: 16710047]
14. Corsico B, Liou HL, Storch J (2004) The alpha-helical domain of liver fatty acid binding protein is responsible for the diffusion-mediated transfer of fatty acids to phospholipid membranes. Biochemistry 43:3600–3607 [PubMed: 15035630]
15. Thumser AE, Storch J (2000) Liver and intestinal fatty acid-binding proteins obtain fatty acids from phospholipid membranes by different mechanisms. J Lipid Res 41:647–656 [PubMed: 10744786]
16. Storch J, Thumser AE (2000) The fatty acid transport function of fatty acid-binding proteins. Biochim Biophys Acta 1486:28–44 [PubMed: 10856711]
17. Qian J, Atkinson J, Manor D (2006) Biochemical consequences of heritable mutations in the alpha-tocopherol transfer protein. Biochemistry 45:8236–8242 [PubMed: 16819822]
18. Qian J, Morley S, Wilson K, Nava P, Atkinson J, Manor D (2005) Intracellular trafficking of vitamin E in hepatocytes: the role of tocopherol transfer protein. J Lipid Res 46:2072–2082 [PubMed: 16024914]
19. Nava P, Cecchini M, Chirico S, Gordon H, Morley S, Manor D, Atkinson J (2006) Preparation of fluorescent tocopherols for use in protein binding and localization with the alpha-tocopherol transfer protein. Bioorg Med Chem 14:3721–3736 [PubMed: 16481173]
20. Morley S, Panagabko C, Shineman D, Mani B, Stocker A, Atkinson J, Manor D (2004) Molecular determinants of heritable vitamin E deficiency. Biochemistry 43:4143–4149 [PubMed: 15065857]
21. Schroeder F, Barenholz Y, Gratton E, Thompson TE (1987) A fluorescence study of dehydroergosterol in phosphatidylcholine bilayer vesicles. Biochemistry 26:2441–2448 [PubMed: 3607026]
22. Konigsberg PJ, Debrick JE, Pawlowski TJ, Staerz UD (1999) Liposome encapsulated aurothiomalate reduces collagen-induced arthritis in DBA/1 J mice. Biochim Biophys Acta 1421:149–162 [PubMed: 10561480]
23. Massey JB, Bick DH, Pownall HJ (1997) Spontaneous transfer of monoacyl amphiphiles between lipid and protein surfaces. Biophys J 72:1732–1743 [PubMed: 9083677]
24. Morley S, Cross V, Cecchini M, Nava P, Atkinson J, Manor D (2006) Utility of a fluorescent vitamin E analogue as a probe for tocopherol transfer protein activity. Biochemistry 45:1075–1081 [PubMed: 16430203]

25. Panagabko C, Morley S, Hernandez M, Cassolato P, Gordon H, Parsons R, Manor D, Atkinson J (2003) Ligand specificity in the CRAL-TRIO protein family. Biochemistry 42:6467–6474 [PubMed: 12767229]
26. Falomir-Lockhart LJ, Laborde L, Kahn PC, Storch J, Corsico B (2006) Protein–membrane interaction and fatty acid transfer from intestinal fatty acid-binding protein to membranes. Support for a multistep process. J Biol Chem 281:13979–13989 [PubMed: 16551626]
27. Atkinson J, Epand RF, Epand RM (2008) Tocopherols and tocotrienols in membranes: a critical review. Free Radic Biol Med 44:739–764 [PubMed: 18160049]
28. Morley S, Cecchini M, Zhang W, Virgulti A, Noy N, Atkinson J, Manor D (2008) Mechanisms of ligand transfer by the hepatic tocopherol transfer protein. J Biol Chem 283:17797–17804 [PubMed: 18458085]
29. Liou HL, Storch J (2001) Role of surface lysine residues of adipocyte fatty acid-binding protein in fatty acid transfer to phospholipid vesicles. Biochemistry 40:6475–6485 [PubMed: 11371211]
30. Smith ER, Storch J (1999) The adipocyte fatty acid-binding protein binds to membranes by electrostatic interactions. J Biol Chem 274:35325–35330 [PubMed: 10585398]
31. Herr FM, Aronson J, Storch J (1996) Role of portal region lysine residues in electrostatic interactions between heart fatty acid binding protein and phospholipid membranes. Biochemistry 35:1296–1303 [PubMed: 8573586]
32. Herr FM, Matarese V, Bernlohr DA, Storch J (1995) Surface lysine residues modulate the collisional transfer of fatty acid from adipocyte fatty acid binding protein to membranes. Biochemistry 34:11840–11845 [PubMed: 7547918]
33. Herr FM, Li E, Weinberg RB, Cook VR, Storch J (1999) Differential mechanisms of retinoid transfer from cellular retinol binding proteins types I and II to phospholipid membranes. J Biol Chem 274:9556–9563 [PubMed: 10092641]
34. Huang C (1969) Studies on phosphatidylcholine vesicles. Formation and physical characteristics, Biochemistry 8:344–352 [PubMed: 5777332]
35. Szoka F Jr, Papahadjopoulos D (1980) Comparative properties and methods of preparation of lipid vesicles (liposomes). Annu Rev Biophys Bioeng 9:467–508 [PubMed: 6994593]
36. Hosomi A, Arita M, Sato Y, Kiyose C, Ueda T, Igarashi O, Arai H, Inoue K (1997) Affinity for alpha tocopherol transfer protein as a determinant of the biological activities of vitamin E analogs. FEBS Lett 409:105–108 [PubMed: 9199513]
37. Parker RS, Sontag TJ, Swanson JE, McCormick CC (2004) Discovery, characterization, and significance of the cytochrome p450 omega-hydroxylase pathway of vitamin E catabolism. In: Kelly F, Meydani M, Packer L (eds) Vitamin E and Health. NYAS, New York, pp 13–21
38. Sontag TJ, Parker RS (2007) Influence of major structural features of tocopherols and tocotrienols on their omega-oxidation by tocopherol-omega-hydroxylase. J Lipid Res 48:1090–1098 [PubMed: 17284776]
39. Wagner KH, Kamal-Eldin A, Elmadfa I (2004) Gamma-tocopherol—an underestimated vitamin? Ann Nutr Metab 48:169–188 [PubMed: 15256801]
40. Traber MG (2007) Vitamin E bioavailability. In: Preedy VR, Watson RR (eds) The encyclopedia of vitamin E. CABI International, Wallingford
41. Traber MG, Burton GW, Hamilton RL (2004) Vitamin E trafficking. In: Kelly F, Meydani M, Packer L (eds) Vitamin E and health. NYAS, New York, pp 1–12
42. Mulgrew-Nesbitt A, Diraviyam K, Wang J, Singh S, Murray P, Li Z, Rogers L, Mirkovic N, Murray D (2006) The role of electro-statics in protein–membrane interactions. Biochim Biophys Acta 1761:812–826 [PubMed: 16928468]
43. Schumann RR, Latz E (2000) Lipopolysaccharide-binding protein. Chem Immunol 74:42–60 [PubMed: 10608081]
44. Lamping N, Hoess A, Yu B, Park TC, Kirschning CJ, Pfeil D, Reuter D, Wright SD, Herrmann F, Schumann RR (1996) Effects of site-directed mutagenesis of basic residues (Arg 94, Lys 95, Lys 99) of lipopolysaccharide (LPS)-binding protein on binding and transfer of LPS and subsequent immune cell activation. J Immunol 157:4648–4656 [PubMed: 8906845]
45. Schultz H, Weiss JP (2007) The bactericidal/permeability-increasing protein (BPI) in infection and inflammatory disease. Clin Chim Acta 384:12–23 [PubMed: 17678885]

46. Gazzano-Santoro H, Parent JB, Conlon PJ, Kasler HG, Tsai CM, Lill-Elghanian DA, Hollingsworth RI (1995) Characterization of the structural elements in lipid A required for binding of a recombinant fragment of bactericidal/permeability-increasing protein rBPI23. Infect Immun 63:2201–2205 [PubMed: 7768599]
47. Desrumaux C, Labeur C, Verhee A, Tavernier J, Vandekerckhove J, Rosseneu M, Peelman F (2001) A hydrophobic cluster at the surface of the human plasma phospholipid transfer protein is critical for activity on high density lipoproteins. J Biol Chem 276:5908–5915 [PubMed: 11083872]
48. Bollinger JG, Diraviyam K, Ghomashchi F, Murray D, Gelb MH (2004) Interfacial binding of bee venom secreted phospholipase A2 to membranes occurs predominantly by a nonelectrostatic mechanism. Biochemistry 43:13293–13304 [PubMed: 15491136]
49. Pan YH, Yu BZ, Singer AG, Ghomashchi F, Lambeau G, Gelb MH, Jain MK, Bahnson BJ (2002) Crystal structure of human group × secreted phospholipase A2. Electrostatically neutral interfacial surface targets zwitterionic membranes. J Biol Chem 277:29086–29093 [PubMed: 12161451]
50. Winget JM, Pan YH, Bahnson BJ (2006) The interfacial binding surface of phospholipase A2s. Biochim Biophys Acta 1761:1260–1269 [PubMed: 16962825]
51. Kutateladze TG (2007) Mechanistic similarities in docking of the FYVE and PX domains to phosphatidylinositol 3-phosphate containing membranes. Prog Lipid Res 46:315–327 [PubMed: 17707914]
52. Kutateladze TG, Capelluto DG, Ferguson CG, Cheever ML, Kutateladze AG, Prestwich GD, Overduin M (2004) Multivalent mechanism of membrane insertion by the FYVE domain. J Biol Chem 279:3050–3057 [PubMed: 14578346]
53. De Matteis MA, D'Angelo G (2007) The role of the phosphoinositides at the Golgi complex. Biochem Soc Symp 74:107–116
54. De Matteis MA, Godi A (2004) PI-lotting membrane traffic. Nat Cell Biol 6:487–492 [PubMed: 15170460]
55. Arai H (2006) Molecular mechanisms of α-tocopherol transfer protein (α-TTP)-dependent *α*-tocopherol transfer in hepatocytes. FASEB J 20:LB44
56. Kozlovsky Y, Chernomordik LV, Kozlov MM (2002) Lipid intermediates in membrane fusion: formation, structure, and decay of hemifusion diaphragm. Biophys J 83:2634–2651 [PubMed: 12414697]
57. Kozlovsky Y, Kozlov MM (2003) Membrane fission: model for intermediate structures. Biophys J 85:85–96 [PubMed: 12829467]
58. Burger KN (2000) Greasing membrane fusion and fission machineries. Traffic 1:605–613 [PubMed: 11208148]
59. Morris R, Cox H, Mombelli E, Quinn PJ (2004) Rafts, little caves and large potholes: how lipid structure interacts with membrane proteins to create functionally diverse membrane environments. Subcell Biochem 37:35–118 [PubMed: 15376618]
60. Qian JH, Morley S, Wilson K, Nava P, Atkinson J, Manor D (2005) Intracellular trafficking of vitamin E in hepatocytes: the role of tocopherol transfer protein. J Lipid Res 46:2072–2082 [PubMed: 16024914]
61. Gruenberg J (2001) The endocytic pathway: a mosaic of domains. Nat Rev Mol Cell Biol 2:721–730 [PubMed: 11584299]
62. Gruenberg J (2003) Lipids in endocytic membrane transport and sorting. Curr Opin Cell Biol 15:382–388 [PubMed: 12892777]
63. Gruenberg J, Stenmark H (2004) The biogenesis of multivesicular endosomes. Nat Rev Mol Cell Biol 5:317–323 [PubMed: 15071556]
64. Ganley IG, Carroll K, Bittova L, Pfeffer S (2004) Rab9 GTPase regulates late endosome size and requires effector interaction for its stability. Mol Biol Cell 15:5420–5430 [PubMed: 15456905]
65. Mullock BM, Hinton RH, Peppard JV, Slot JW, Luzio JP (1987) The preparative isolation of endosome fractions: a review. Cell Biochem Funct 5:235–243 [PubMed: 2890445]
66. Genisset C, Puhar A, Calore F, de Bernard M, Dell'Antone P, Montecucco C (2007) The concerted action of the Helicobacter pylori cytotoxin VacA and of the v-ATPase proton pump induces swelling of isolated endosomes. Cell Microbiol 9:1481–1490 [PubMed: 17253977]

67. Kobayashi T, Beuchat MH, Lindsay M, Frias S, Palmiter RD, Sakuraba H, Parton RG, Gruenberg J (1999) Late endosomal membranes rich in lysobisphosphatidic acid regulate cholesterol transport. Nat Cell Biol 1:113–118 [PubMed: 10559883]
68. Kobayashi T, Stang E, Fang KS, de Moerloose P, Parton RG, Gruenberg J (1998) A lipid associated with the antiphospholipid syndrome regulates endosome structure and function. Nature 392:193–197 [PubMed: 9515966]
69. Subra C, Laulagnier K, Perret B, Record M (2007) Exosome lipidomics unravels lipid sorting at the level of multivesicular bodies. Biochimie 89:205–212 [PubMed: 17157973]
70. Laulagnier K, Grand D, Dujardin A, Hamdi S, Vincent-Schneider H, Lankar D, Salles JP, Bonnerot C, Perret B, Record M (2004) PLD2 is enriched on exosomes and its activity is correlated to the release of exosomes. FEBS Lett 572:11–14 [PubMed: 15304316]
71. Horiguchi M, Arita M, Kaempf-Rotzoll DE, Tsujimoto M, Inoue K, Arai H (2003) pH-dependent translocation of alpha-tocopherol transfer protein (alpha-TTP) between hepatic cytosol and late endosomes. Genes to Cells 8:789–800 [PubMed: 14531858]
72. Matsuo H, Chevallier J, Mayran N, Le Blanc I, Ferguson C, Faure J, Blanc NS, Matile S, Dubochet J, Sadoul R, Parton RG, Vilbois F, Gruenberg J (2004) Role of LBPA and Alix in multivesicular liposome formation and endosome organization. Science 303:531–534 [PubMed: 14739459]
73. van der Goot FG, Gruenberg J (2006) Intra-endosomal membrane traffic. Trends Cell Biol 16:514–521 [PubMed: 16949287]
74. Hayakawa T, Makino A, Murate M, Sugimoto I, Hashimoto Y, Takahashi H, Ito K, Fujisawa T, Matsuo H, Kobayashi T (2007) pH-dependent formation of membranous cytoplasmic body-like structure of ganglioside G(M1)/bis(monoacylglycero)phosphate mixed membranes. Biophys J 92:L13–L16 [PubMed: 17056735]
75. Cheruku SR, Xu Z, Dutia R, Lobel P, Storch J (2006) Mechanism of cholesterol transfer from the Niemann-Pick type C2 protein to model membranes supports a role in lysosomal cholesterol transport. J Biol Chem 281:31594–31604 [PubMed: 16606609]
76. Kleinfeld AM, Storch J (1993) Transfer of long-chain fluorescent fatty acids between small and large unilamellar vesicles. Biochemistry 32:2053–2061 [PubMed: 8448164]
77. Davies JK, Thumser AE, Wilton DC (1999) Binding of recombinant rat liver fatty acid-binding protein to small anionic phospholipid vesicles results in ligand release: a model for interfacial binding and fatty acid targeting. Biochemistry 38:16932–16940 [PubMed: 10606528]
78. Huang H, Ball JM, Billheimer JT, Schroeder F (1999) Interaction of the N-terminus of sterol carrier protein 2 with membranes: role of membrane curvature. Biochem J 344(Pt 2):593–603 [PubMed: 10567245]
79. Rao CS, Lin X, Pike HM, Molotkovsky JG, Brown RE (2004) Glycolipid transfer protein mediated transfer of glycosphingolipids between membranes: a model for action based on kinetic and thermodynamic analyses. Biochemistry 43:13805–13815 [PubMed: 15504043]
80. Mesmin B, Drin G, Levi S, Rawet M, Cassel D, Bigay J, Antonny B (2007) Two lipid-packing sensor motifs contribute to the sensitivity of ArfGAP1 to membrane curvature. Biochemistry 46:1779–1790 [PubMed: 17253781]
81. Bigay J, Casella JF, Drin G, Mesmin B, Antonny B (2005) ArfGAP1 responds to membrane curvature through the folding of a lipid packing sensor motif. Embo J 24:2244–2253 [PubMed: 15944734]
82. Wootan MG, Storch J (1994) Regulation of fluorescent fatty acid transfer from adipocyte and heart fatty acid binding proteins by acceptor membrane lipid composition and structure. J Biol Chem 269:10517–10523 [PubMed: 8144637]
83. Kucerka N, Nagle JF, Sachs JN, Feller SE, Pencer J, Jackson A, Katsaras J (2008) Lipid bilayer structure determined by the simultaneous analysis of neutron and X-ray scattering data. Biophys J 95:2356–2367 [PubMed: 18502796]
84. Lomize AL, Pogozheva ID, Lomize MA, Mosberg HI (2007) The role of hydrophobic interactions in positioning of peripheral proteins in membranes. BMC Struct Biol 7:44 [PubMed: 17603894]
85. Lomize AL, Pogozheva ID, Lomize MA, Mosberg HI (2006) Positioning of proteins in membranes: a computational approach. Protein Sci 15:1318–1333 [PubMed: 16731967]

86. Lomize MA, Lomize AL, Pogozheva ID, Mosberg HI (2006) OPM: orientations of proteins in membranes database. Bioinformatics 22:623–625 [PubMed: 16397007]

87. Bhardwaj N, Stahelin RV, Langlois RE, Cho W, Lu H (2006) Structural bioinformatics prediction of membrane-binding proteins. J Mol Biol 359:486–495 [PubMed: 16626739]

88. Bhardwaj N, Stahelin RV, Zhao G, Cho W, Lu H (2007) MeTaDoR: a comprehensive resource for membrane targeting domains and their host proteins. Bioinformatics 23:3110–3112 [PubMed: 17720983]

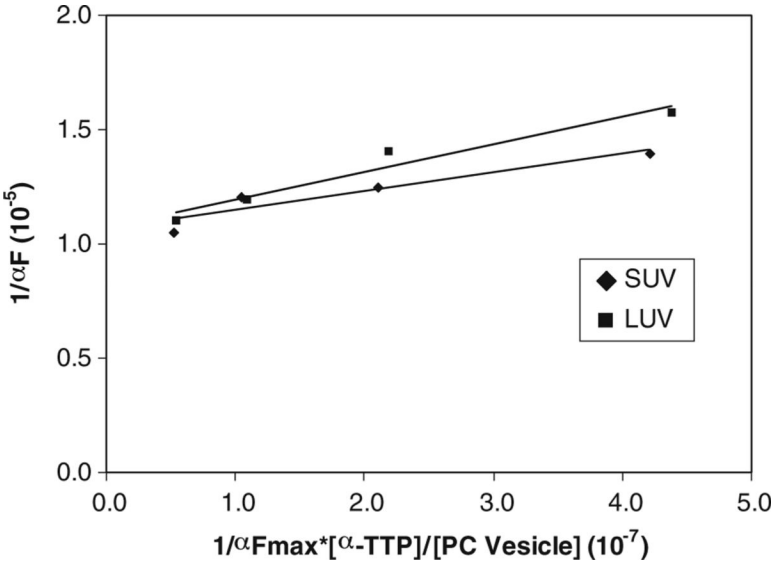

Fig. 1.

Partitioning of NBD-Toc between α-TTP and SUVs or LUVs. Titration of NBD-Toc (0.225 μM) bound to α-TTP (2 μM) with PC SUVs (*filled diamonds*) or LUVs (*filled squares*) at a concentration of 50, 100, 200 and 400 μM. The change in fluorescence intensity between NBD-Toc bound to α-TTP and vesicles at each lipid concentration is expressed as ΔF. The partition coefficients determined for this particular experiment are 0.122 and 0.082 for SUVs and LUVs, respectively

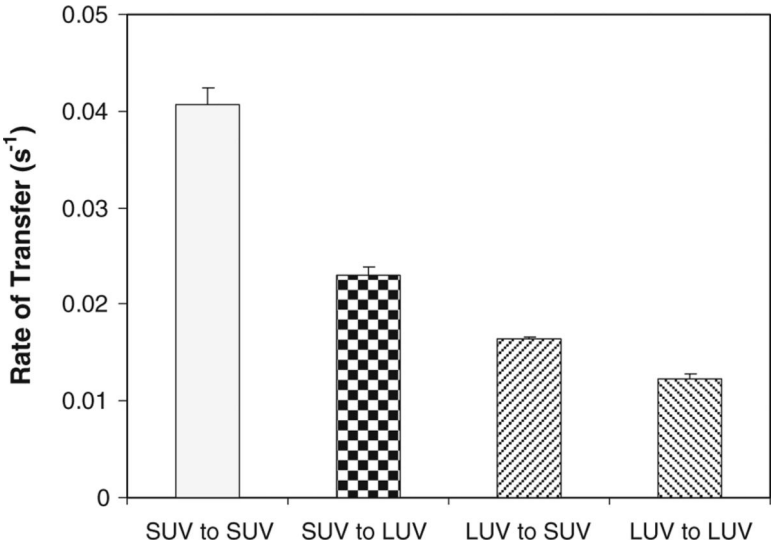

Fig. 2.

Intervesicle transfer of NBD-Toc from donor vesicles to acceptor vesicles. 1 μM NBD-Toc incorporated in 100 μM donor PC SUVs or LUVs was transferred to 100 μM acceptor bovine liver PC SUVs or LUVs containing 3% TRITC-PE. Data shown represent an average of six determinations ± the standard deviation

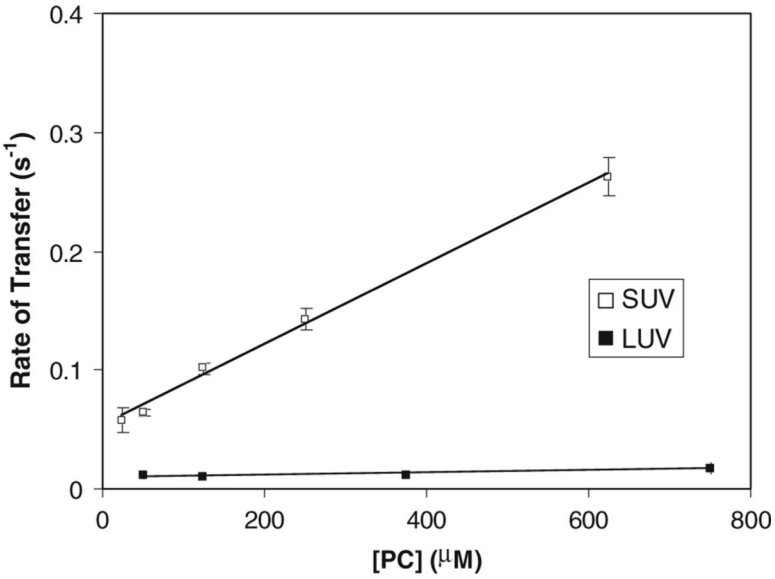

Fig. 3.

Effect of lipid concentration on the rate of NBD-Toc transfer from α-TTP to PC SUVs and LUVs. Transfer of 0.125 μM NBD-Toc from 1.25 lM α-TTP to SUVs (*open squares*) or LUVs (*filled squares*) at the indicated concentration was monitored at room temperature. Results are the average of three curves ± the standard deviation

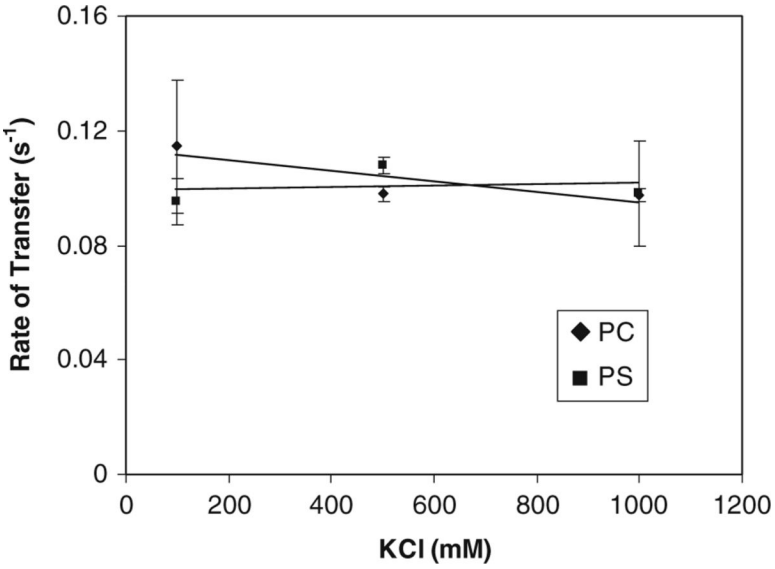

Fig. 4.

Effect of ionic strength on the rate of NBD-Toc transfer to PC or PS SUVs. 0.225 μM NBD-Toc transferred from 2 μM α-TTP to 100 μM PC SUVs (*filled circles*) or PC SUVs containing 15% PS (*filled squares*) in the presence of an increasing concentration of KCl. Data shown represents an average ± the standard deviation, $n = 12$ for PC at 100 mM KCl, $n = 3$ for other conditions tested. The data shown are compiled from separate experiments with different protein and lipid preparations

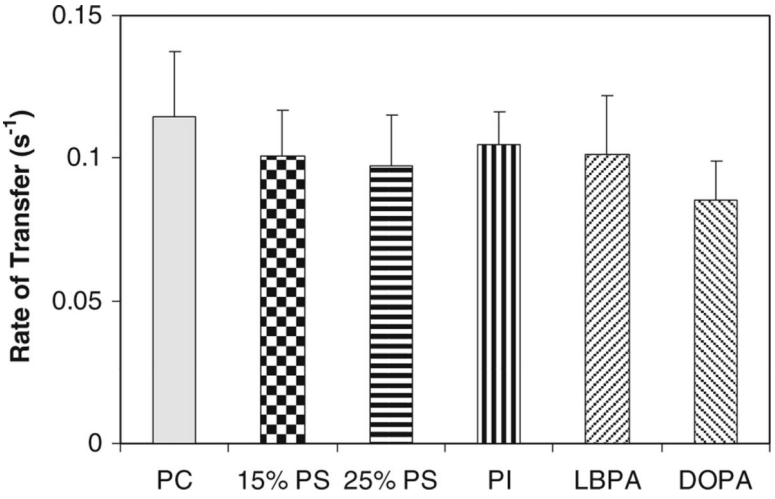

Fig. 5.

NBD-Toc transfer from α-TTP to anionic SUVs. Transfer of 0.225 μM NBD-Toc from 2 μM α-TTP to 100 μM bovine liver PC SUVs containing 15 mol% of PS, PI, LBPA and DOPA or 25 mol% of PS. Results are the average ± the standard deviation, $n = 3$ for PI, PS, LBPA and DOPA and $n = 12$ for PC only controls. No statistical differences were observed between PC vesicles and those of variant lipid composition, as assessed by unpaired t tests

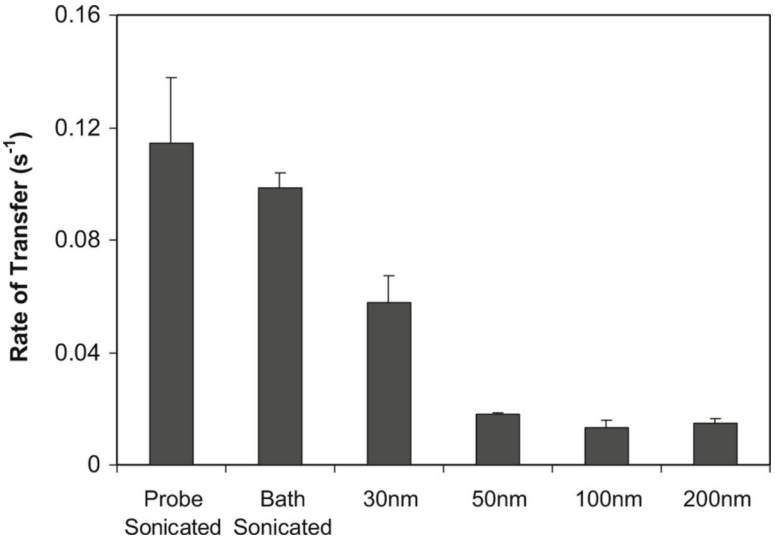

Fig. 6.

Effect of vesicle size on the rate of NBD-Toc transfer from α-TTP. PC vesicles were prepared by probe sonication, bath sonication or extrusion. The transfer of NBD-Toc (0.225 μM) from 2 μM α-TTP to 100 μM vesicles of various sizes was monitored. Data shown represents the average ± the standard deviation $n = 12$ for the probe-sonicated PC SUV, $n = 18$ for 100 nm PC LUV, $n = 3$ for other conditions tested. Vesicles sizes represent the nominal pore size of the filters used for extrusion. For full details on the vesicles size distribution see “Materials and Methods”

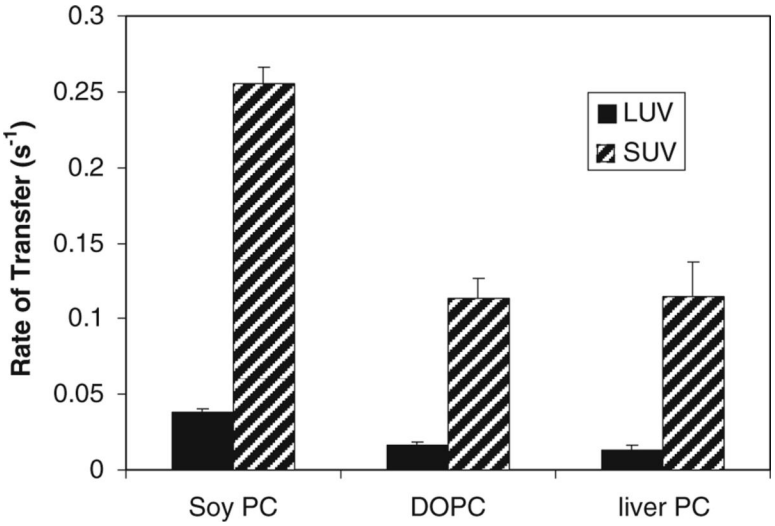

Fig. 7.

Effect of lipid saturation on α-TTP mediated NBD-Toc transfer. Transfer of 0.225 μM NBD-Toc from 2 μM α-TTP to 100 μM PC LUVs (*closed bar*) and SUVs (*hatched bar*) of soy PC, DOPC or liver PC was monitored. Data shown represents an average ± the standard deviation, $n = 3$ for soy PC and DOPC, $n = 12$ for PC SUVs and $n = 18$ for PC LUVs